Available online at www.sciencedirect.com
ScienceDirect
Solid State Sciences 10 (2008) 1947–1950
www.elsevier.com/locate/ssscie

Electrical property evolution in the graphitization process of activated carbon by high-pressure sintering

J.G. Zhao*, L.X. Yang, F.Y. Li, R.C. Yu, C.Q. Jin

Beijing National Lab for Condensed Matter Physics, Institute of Physics, Chinese Academy of Sciences, Beijing 100080, PR China

Received 6 November 2007; received in revised form 25 February 2008; accepted 25 March 2008
Available online 8 April 2008

Abstract

Activated carbon was treated at 5.0 GPa up to 1600 °C, and the electrical property evolution in the graphitization process was investigated. The change of structure results in the corresponding electrical property transition. For the samples at low high-pressure sintering temperature, the variable-range hopping is the main electrical transportation mechanism. The graphitized activated carbon is a semimetal while the high-pressure sintering temperature is lower than 1300 °C and behaves non-Fermi-liquid property at higher sintering temperature. The ratio of resistivity at ~5.0 and ~300.0 K versus high-pressure sintering temperature is drastically decreasing near the graphitization temperature, which indicates that the insulator–metal transition occurs in the sintering temperature range of 900–1000 °C.

Keywords: Activated carbon; High pressure; Graphitization; Electrical properties

1. Introduction

The forms of carbon include the crystalline phase of graphite, diamond and fullerence, and many amorphous materials [1]. Activated carbon, as one of non-crystalline carbon, is composed of micrographites in nanometer scale with short-range order [1]. The micrographite is formed with the stack of nano-sized graphitic sheets. Recently, some interesting physical phenomena were found on carbon-based materials, e.g. highly oriented pyrolytic graphite [2], electron-doped C_{60} [3], glassy carbon [4], etc. It is thought that these phenomena could be related to the microstructure in these materials. The sheets and micrographites have other special properties in electrical transportation, optical spectra, field emission, etc. [5–7]. So the study for activated carbon is helpful to understand the properties of nano-sized materials.

Activated carbon could become graphite under high temperature, like most amorphous carbon materials [8]. The graphitization temperature would reach above 2500 °C at ambient condition [9]. High pressure can significantly reduce the graphitization temperature and substantially accelerate the kinetics of transition of activated carbon and other non-crystalline carbon [10]. Inagaki et al. have reported that non-graphitized carbons can become graphite at ~1500–1700 °C and 0.5 GPa [11]. The current-induced movement of Fe particles could transform the amorphous carbon nanowires into the graphitized carbon nanowires [12], which affects the purity of samples. Activated carbon treated under high pressure and high temperature would be pure and useful for further research and application. We have treated activated carbon powder by high-pressure sintering with the pressure up to 5 GPa, and researched the graphitization process [13]. In this paper, we have measured the temperature dependences of resistivity to study the electrical property evolution in the graphitization process of activated carbon.

2. Experimental

We performed the high-pressure and high-temperature treatments on activated carbon by using a conventional cubic-anvil

* Corresponding author. Tel.: +86 10 82648041; fax: +86 10 82640223.
E-mail address: zhaojinggeng@163.com (J.G. Zhao).

1293-2558/$ - see front matter © 2008 Elsevier Masson SAS. All rights reserved.
doi:10.1016/j.solidstatesciences.2008.03.022

type high-pressure facility [13]. The treating process was carried out at 5.0 GPa and 100–1600 °C for 5–10 min. Here the samples are represented as HPHT*n*, where *n* is equal to the high-pressure sintering temperature. For example, HPHT1200 denotes activated carbon treated at 1200 °C and 5.0 GPa. The structures of these samples were checked by the powder X-ray diffraction (XRD) technology with Cu Kα radiation at room temperature, using a Rigaku diffractometer (MXP-AHP18) for $2\theta = 10–90°$. According to the peak intensity evolution, as shown in Fig. 1, the graphitization process can be distinctly viewed into three regions: the non-graphitization region, the near-graphitization region, and the graphitization region, which correspond to activated carbon treated below 900, 1000–1100 and above 1200 °C, respectively. The measurements of temperature dependences of electrical resistivity in the temperature range of 5.0–300.0 K were performed by using the standard four-probe method with Ag paste contacts on an Oxford Maglab measuring system.

3. Results and discusion

The electrical property transition of activated carbon treated under high pressure and high temperature corresponds to the structural evolution very well. Fig. 2 shows the temperature dependences of electrical resistivity for activated carbon treated below 800 °C. The one-dimensional variable-range hopping conduction mechanism exists in HPHT300–800 that is made of dispersive or merged carbon grains. The relationships of resistivity versus temperature follow the law:

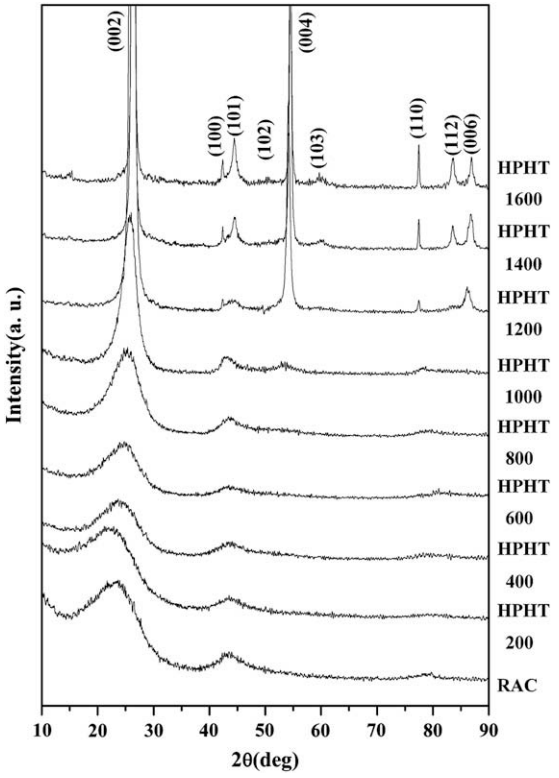

Fig. 1. The XRD patterns for activated carbon prepared at 5.0 GPa and different temperatures. The RAC represents the raw activated carbon.

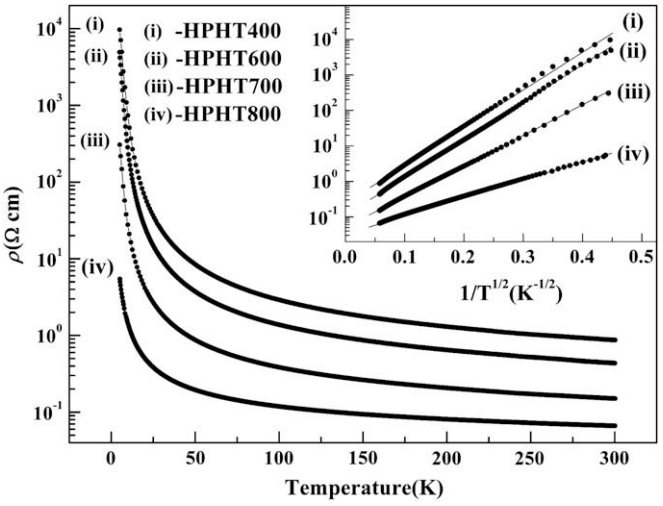

Fig. 2. The temperature dependences of electrical resistivity for activated carbon treated below 800 °C. The inset shows the relationships of electrical resistivity versus $T^{-1/2}$.

$$\rho(T) = \rho_0 \exp\left[(T_0/T)^{1/2}\right], \tag{1}$$

where ρ_0 is the resistivity at $T = \infty$. The inset of Fig. 2 shows the linear relationship of $\log \rho$ versus $T^{-1/2}$. The T_0 of HPHT300–800 is obtained through Eq. (1), and the relationship of T_0 versus high-pressure sintering temperature is shown in Fig. 3a. Through the formula:

$$T_0 = \left(6e^2/\pi k_B\right)^*(1/4\pi\varepsilon_r\varepsilon_0)^*(1/\xi), \tag{2}$$

the localization length ξ of the wave function is achieved, assuming the dielectric constant ε_r is equal to 10 [14,15] as shown in Fig. 3b. The ξ takes a value similar to the *ab*-plane size L_a of the graphitic granules [13].

Fig. 4 shows the temperature dependence of electrical resistivity for HPHT900, with the three-dimensional variable-range

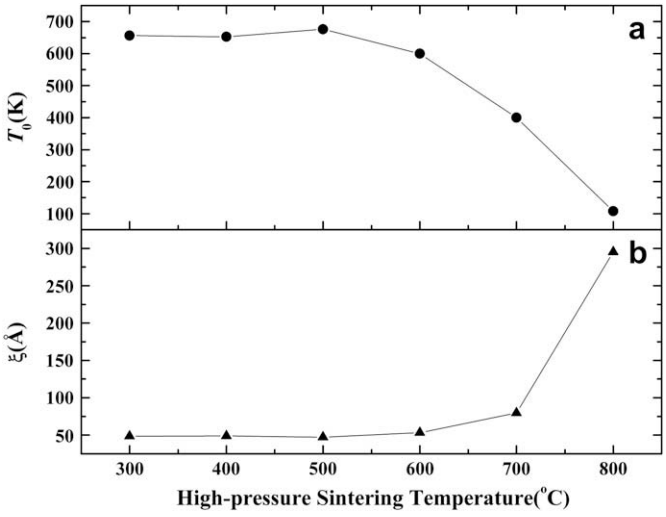

Fig. 3. The high-pressure sintering temperature dependences of (a) T_0 and (b) localization length ξ in the range 300–800 °C.

hopping conduction mechanism. The relationship of resistivity versus temperature below 140 K follows the law:

$$\rho(T) = \rho_0 \exp\left[(T_0/T)^{1/4}\right], \tag{3}$$

The inset of Fig. 4 shows the linear relationship of log ρ versus $T^{-1/4}$. As we know, the one-dimensional hopping of electrons exists widely in activated carbon sintered under ambient pressure [14–16], but the three-dimensional hopping has not been found in previous results although it exists in many non-crystalline semiconductor materials. There are many insulating regions (carbon grains) in activated carbon, and the electrical transportation between these tiny regions depends mainly on the hopping, which is the governed conduction mechanism in these samples [17]. With increasing high-pressure sintering temperature, small insulating regions merge into larger ones. The conduction mechanism transfers to three-dimension hopping from one-dimension one while these insulating regions become larger but do not form pre-graphitic grains in HPHT900.

In the near-graphitization region, the relationship of electrical resistivity versus temperature is nearly linear above about 100 K. Fig. 4 shows the result of HPHT1000. The conduction mechanism is intervenient the semiconductor and semimetal. The appearance of honeycomb-like textures shows that the structure of activated carbon changes dramatically and micrographites connect to each other more closely [13], which weakens the variable-range hopping conduction mechanism and strengthens the semimetal property of samples.

Fig. 5 shows the temperature dependence of relative electrical resistivity for the graphitized activated carbon. HPHT1200 and HPHT1300 behave common semimetal property in conduction mechanism like polycrystalline graphite, with linear relationship of resistivity versus temperature. HPHT1400–1600 exhibits special electrical property. The relationship of resistivity versus temperature below 80 K of these samples follows the law:

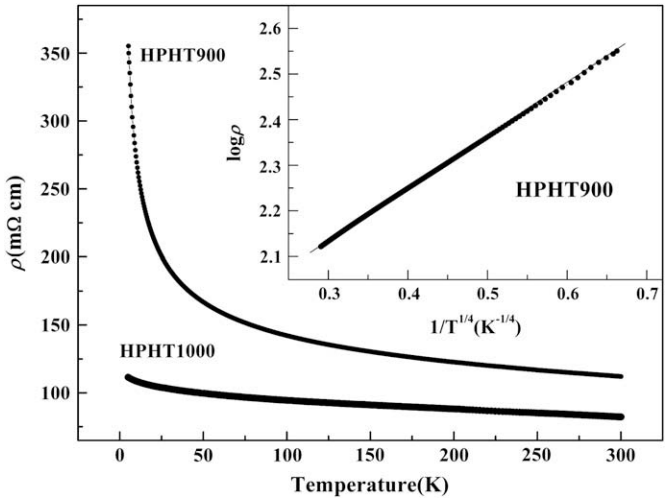

Fig. 4. The temperature dependences of electrical resistivity for HPHT900 and HPHT1000. The inset shows the relationships of electrical resistivity versus $T^{-1/4}$ for HPHT900.

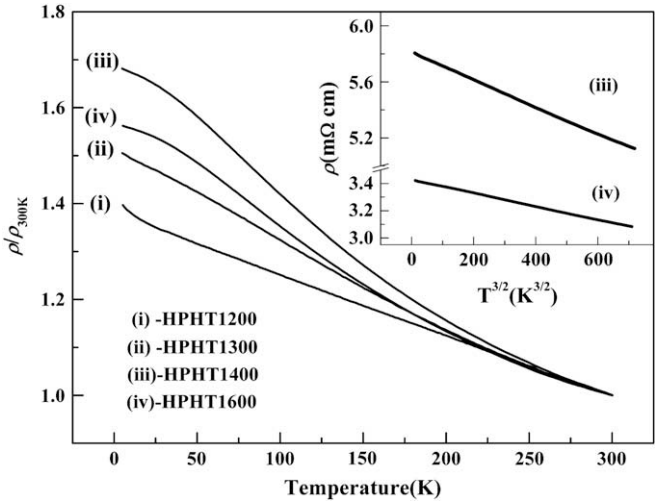

Fig. 5. The temperature dependences of electrical resistivity for activated carbon treated above 1200 °C. The inset shows the relationships of electrical resistivity versus $T^{3/2}$ for HPHT1400 and HPHT1600.

$$\rho(T) = \rho_0 + AT^{3/2}, \tag{4}$$

where ρ_0 is the resistivity at $T = 0$ and A is a negative constant. The inset of Fig. 5 shows the linear relationships of resistivity versus $T^{3/2}$ for the sample HPHT1400 and HPHT1600. The conduction mechanism under low temperature is similar to that of $Y_{0.8}U_{0.2}Pd_3$ alloy [18], which indicates that there may be a non-Fermi-liquid behavior in our samples. According to our prevenient results [13], there are the disorder structures in the graphitized activated carbon, which are reflected by SEM photographs and Raman spectra. This non-Fermi-liquid behavior is attributed to the disorder structures in the graphitized activated carbon.

Fig. 6 shows the high-pressure sintering temperature dependence of the ratio of resistivity at 5.0 and 300.0 K with

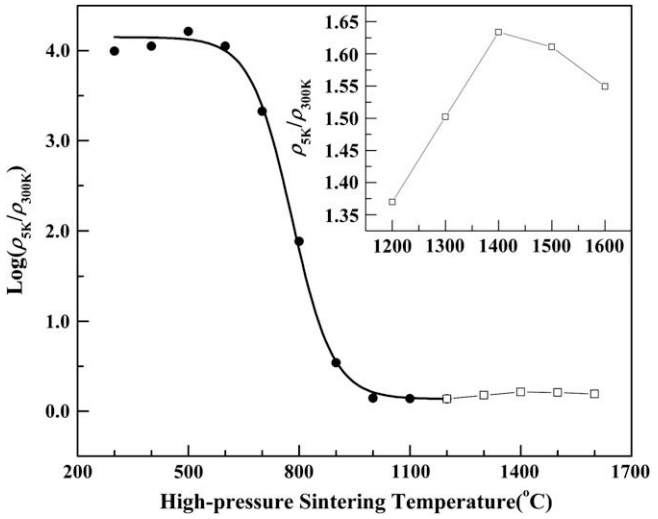

Fig. 6. The high-pressure sintering temperature dependence of the ratio of resistivity at 5.0 and 300.0 K for HPHT300–1600, with the y-axis in logarithmic scale. The black bold line is the Boltzmann fit to these data. The inset shows the relationship of $\rho_{5.0K}/\rho_{300.0K}$ versus high-pressure sintering temperature for the graphitized activated carbon.

the *y*-axis in logarithmic scale for HPHT300–1600. The black bold line is Boltzmann fit to these data. The inset shows the relationship of $\rho_{5.0K}/\rho_{300.0K}$ versus high-pressure sintering temperature for the graphitized activated carbon. The ratio decreases drastically between 700 and 1000 °C. The insulator–metal transition occurs in the high-pressure sintering temperature range of 900–1000 °C, which is less than that of activated carbon sintered under ambient pressure [16].

4. Conclusions

In the graphitization process of activated carbon treated by high-pressure sintering, the electrical properties show a corresponding relationship with a variety of structural features. The continuous occurrence of variable-range hopping, the approximatively linear ρ–T relationship, and semimetal conduction mechanism, accords with three regions in the graphitization process. The insulator–metal transition occurs between non-graphitization region and near-graphitization region.

Acknowledgements

This work was supported by NSF and Ministry of Science and Technology of China through the research projects.

References

[1] J. Robertson, Adv. Phys. 35 (1986) 317.
[2] H. Kempa, Y. Kopelevich, F. Mrowka, A. Setzer, J.H.S. Torres, R. Höhne, P. Esquinazi, Solid State Commun. 115 (2000) 539.
[3] A.F. Hebard, M.J. Rosseinsky, R.C. Haddon, D.W. Murphy, S.J. Glarum, T.T.M. Palstra, A.P. Ramirez, A.R. Kortan, Nature 350 (1991) 600.
[4] X. Wang, Z.X. Liu, Y.L. Zhang, F.Y. Li, R.C. Yu, C.Q. Jin, J. Phys.: Condens. Matter 14 (2002) 10265.
[5] K. Nakada, M. Igami, M.Fujita, J. Phys. Soc. Jpn. 67 (1998) 2388.
[6] K. Wakabayashi, M. Fujita, H. Ajiki, M. Sigrist, Phys. Rev. B 59 (1999) 8271.
[7] C.W. Chiu, F.L. Shyu, C.P. Chang, R.B. Chen, M.F. Lin, J. Phys. Soc. Jpn. 72 (2003) 170.
[8] R.E. Franklin, Proc. R. Soc. London, Ser. A 209 (1951) 196.
[9] Y. Hishiyama, M. Inagaki, S. Kimura, S. Yamada, Carbon 12 (1974) 249.
[10] X. Wang, G.M. Zhang, Y.L. Zhang, F.Y. Li, R.C. Yu, C.Q. Jin, G.T. Zou, Carbon 41 (2003) 188.
[11] M. Inagaki, A. Oberlin, S. de Fonton, High Temp.-High Press. 9 (1977) 453.
[12] C.H. Jin, J.Y. Wang, Q. Chen, L.-M. Peng, J. Phys. Chem. B 110 (2006) 5423.
[13] J.G. Zhao, F.Y. Li, R.C. Yu, C.Q. Jin, unpublished.
[14] A.W.P. Fung, A.M. Rao, K. Kuriyama, M.S. Dresselhaus, G. Dresselhaus, M. Endo, J. Mater. Res. 8 (1993) 489.
[15] A.W.P. Fung, Z.H. Wang, M.S. Dresselhaus, G. Dresselhaus, R.W. Pekala, M. Endo, Phys. Rev. B 49 (1994) 17325.
[16] A.W.P. Fung, M.S. Dresselhaus, M. Endo, Phys. Rev. B 48 (1993) 14953.
[17] K. Kuriyama, M.S. Dresselhaus, J. Mater. Res. 4 (1992) 940.
[18] C.L. Seaman, M.B. Maple, B.W. Lee, S. Ghamaty, M.S. Torikachvili, J.-S. Kang, L.Z. Liu, J.W. Allen, D.L. Cox, Phys. Rev. Lett. 67 (1991) 2882.